

Protonation of CpW(CO)₂(PMe₃)H: Is the Metal or the Hydride the Kinetic Site?

Elizabeth T. Papish,[†] Francis C. Rix,[‡] Nikos Spetseris,[‡] Jack R. Norton,^{*,†} and Robert D. Williams[§]

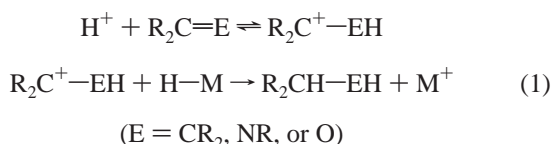
Contribution from the Departments of Chemistry, Columbia University, 3000 Broadway, New York, New York 10027, Colorado State University, Fort Collins, Colorado 80523, and Princeton University, Princeton New Jersey 08544

Received July 3, 2000

Abstract: We have compared the rate at which a proton is transferred to the hydride ligand of CpW(CO)₂(PMe₃)H (**3**) with the rate at which one is transferred to the metal. Qualitative evidence that protonation of the hydride ligand is faster is offered by observation of fast exchange between **3** and CF₃SO₃D and selective broadening of the trans hydride resonance of **3** during exchange with anilinium. Rate constants were obtained by ¹H NMR for H/D exchange between **3** and 4-*tert*-butyl-*N,N*-dimethylanilinium-*N-d*₁ (**5-d**₁); an unusual EIE of 0.19 was observed and explained by location of the vibrational normal modes of **3**, **5**, and their deuterated analogues via IR and Raman spectroscopy. A pK_a of 5.6(1) in CH₃CN was determined for CpW(CO)₂(PMe₃)-H₂⁺ (**4a**) by IR; the importance of homoconjugate pair interactions in protonation equilibria is illustrated and discussed. The exchange rate data and the rate constant for deprotonation of **4a** by 4-*tert*-butyl-*N,N*-dimethylaniline (**6**), combined with the pK_a data, provide quantitative evidence that the kinetic site of protonation of **3** is the hydride ligand.

Introduction

The reaction of transition-metal hydride complexes with protons¹ is important in the catalysis of the reduction of H⁺ to H₂^{2,3} and in ionic hydrogenation reactions.⁴ The latter involve the sequential transfer of H⁺ and H⁻ to olefins, ketones, or imines (eq 1).



One of us,^{1,5c} and others,⁶ have suggested that there will be a kinetic preference for protonating a hydride complex at the hydride ligand rather than the metal center, because reaction at

the former site will involve less geometric and electronic rearrangement.^{1,5,6} The result of hydride ligand protonation will be a dihydrogen complex.^{6,7}

By observing that NEt₃ broadens the hydride resonances of [Cp(dmpe)Ru(H₂)]⁺ but not [Cp(dmpe)RuH₂]⁺,⁸ Heinekey has shown^{6b} that the kinetic acidity of a dihydrogen complex will be greater than that of the corresponding dihydride. Several experiments in the literature suggest that the microscopic reverse is true, i.e., that a dihydrogen intermediate will generally be the kinetic product of the protonation of a hydride complex. Heinekey has observed that Cp^(*)Ru(PPh₃)₂H is protonated at the hydride ligand at low temperature but isomerizes to a metal dihydride upon warming.⁸ In a similar study by Morris et al., when Cp^{*}Ru(dppp)H is protonated at -60 °C, a dihydrogen complex is initially formed, and, at room temperature, the dihydrogen complex slowly isomerizes to the trans dihydride.⁹

Upon protonation of Re(NO)(CO)L₂H₂ with CF₃COOH at low temperature, an intermediate dihydrogen complex is observed by NMR prior to the loss of H₂.¹⁰ A dihydrogen intermediate is observed at low temperature in the protonation

* To whom correspondence should be addressed.

[†] Columbia University.

[‡] Colorado State University.

[§] Princeton University.

(1) For a review of the protonation reactions of transition-metal complexes, see: Kristjánssdóttir, S. S.; Norton, J. R. *Acidity of Hydrido Transition Metal Complexes in Solution*. In *Transition Metal Hydrides*; Dedieu, A., Ed.; VCH: New York, 1991.

(2) Michaile, S.; Hillman, M.; Eisch, J. J. *Organometallics* **1988**, *7*, 1059–1065 and references therein.

(3) (a) Collman, J. P.; Wagenknecht, P. S.; Hembre, R. T.; Lewis, N. S. *J. Am. Chem. Soc.* **1990**, *112*, 1294–1295. (b) Collman, J. P.; Wagenknecht, P. S.; Lewis, N. S. *J. Am. Chem. Soc.* **1992**, *114*, 5665–5673. (c) Collman, J. P.; Wagenknecht, P. S.; Hutchison, J. E. *Angew. Chem., Int. Ed. Engl.* **1994**, *33*, 1537–1554.

(4) (a) Smith, K.; Norton, J. R.; Tilset, M. *Organometallics* **1996**, *15*, 4515–4520. (b) Bullock, R. M.; Song, J. S. *J. Am. Chem. Soc.* **1994**, *116*, 8602–8612. (c) Song, J. S.; Szalda, D. J.; Bullock, R. M.; Lawrie, C. J. C.; Rodkin, M. A.; Norton, J. R. *Angew. Chem., Int. Ed. Engl.* **1992**, *31*, 1233–1235.

(5) (a) Jordan, R. F.; Norton, J. R. *J. Am. Chem. Soc.* **1982**, *104*, 1255–1263. (b) Jordan, R. F.; Norton, J. R. *ACS Symp. Ser.* **1982**, *198*, 403. (c) *Inorganic Reactions and Methods*; Zuckerman, J. J., Ed.; VCH: New York, 1987; p 207.

(6) (a) Jessop, P. G.; Morris, R. H. *Coord. Chem. Rev.* **1992**, *121*, 155. (b) Heinekey, D. M.; Oldham, W. J., Jr. *Chem. Rev.* **1993**, *93*, 913.

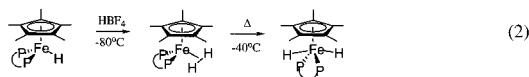
(7) (a) Kubas, G. J. *J. Chem. Soc., Chem. Commun.* **1980**, 61–62. (b) Kubas, G. J. *Comments Inorg. Chem.* **1988**, *7*, 17–40. (c) Kubas, G. J. *Acc. Chem. Res.* **1988**, *21*, 120–128. (d) Crabtree, R. H. *Acc. Chem. Res.* **1990**, *23*, 95–101. (e) Koelle, U. *New J. Chem.* **1992**, *16*, 157–169.

(8) Chinn, M. S.; Heinekey, D. M. *J. Am. Chem. Soc.* **1990**, *112*, 5166–5175.

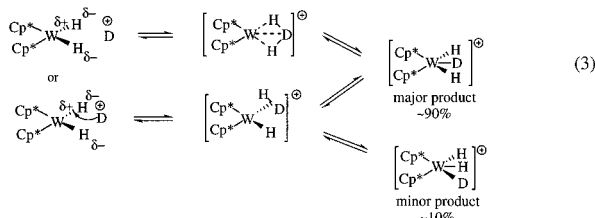
(9) Jia, G.; Lough, A. J.; Morris, R. H. *Organometallics* **1992**, *11*, 161–171.

(10) Feracin, S.; Bürgi, T.; Bakhmutov, V.; Eremenko, I.; Vorontsov, E. V.; Vimenitis, A. B.; Berke, H. *Organometallics* **1994**, *13*, 4194–4213.

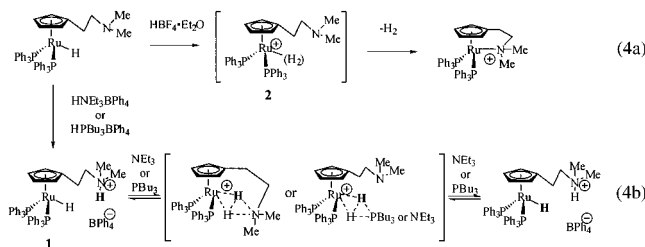
of the iron hydride in eq 2, although a dihydride complex is the sole thermodynamic product.¹¹



When $(\text{CMe}_5)_2\text{WH}_2$ is protonated by $\text{DCI}/\text{D}_2\text{O}$, the major product $([\text{Cp}^*\text{WH}_2\text{D}]^+)$ has a central deuteride ligand.¹² This product cannot result from direct metal protonation because there is no occupied tungsten orbital between the hydride ligands, so the charge-controlled formation of an intermediate $\eta^3\text{-H}_2\text{D}$ or an $(\eta^2\text{-HD})(\text{H})$ dihydrogen complex (eq 3) has been suggested.¹² A kinetic study has confirmed the presence of an intermediate.¹³

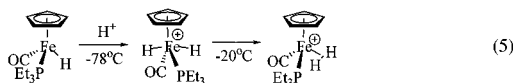


Chaudret has recently shown that the hydride ligand of **1** undergoes intramolecular proton exchange with the ammonium acid (eq 4b).¹⁴ Although the facile loss of H_2 in eq 4a (which



presumably goes through **2**) shows that the cationic H_2 complex **2** cannot be an intermediate in eq 4b, an intermediate like that drawn in eq 4b—with amine coordination stabilizing the coordinated H_2 —remains a possibility.¹⁵ A dihydrogen complex has been observed during the protonation of ruthenium complexes similar to **1**.¹⁶

In an attempt to make a silane σ complex, Brookhart et al. inadvertently generated the iron hydride in eq 5 in situ from



$\text{CpFe}(\text{PEt}_3)(\text{SiEt}_3)\text{CO}$, $\text{H}(\text{OEt}_2)_2^+\text{BAR}'_4^-$, and adventitious H_2O .¹⁷ Protonation, most likely by $\text{Et}_3\text{SiOH}_2^+$ produced in situ, resulted

(11) Hamon, P.; Toupet, L.; Hamon, J.; Lapinte, C. *Organometallics* **1992**, *11*, 1429–1431.

(12) Parkin, G.; Bercaw, J. E. *J. Chem. Soc., Chem. Commun.* **1989**, 255–257.

(13) Henderson, R. A.; Oglieve, K. E. *J. Chem. Soc., Dalton Trans.* **1993**, 3431–3439.

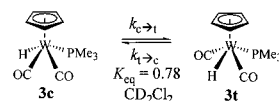
(14) Ayllon, J. A.; Sayers, S. F.; Sabo-Etienne, S.; Donnadieu, B.; Chaudret, B. *Organometallics* **1999**, *18*, 3981–3990.

(15) This possibility is supported by the effect on the proton exchange rate of the base remaining in solution after **1** is formed (Bu_3P makes exchange faster than does Et_3N).¹³ A similar effect (of counterion on H/D exchange rate) was reported by Berke and co-workers with $\text{Re}(\text{NO})(\text{CO})\text{-L}_2\text{H}_2$ in ref 10.

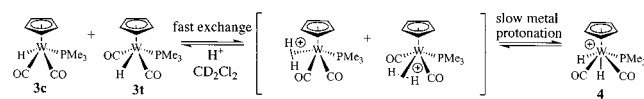
(16) (a) Chu, H. S.; Lau, C. P.; Wong, K. Y.; Wong, W. T. *Organometallics* **1998**, *17*, 2768. (b) Caballero, A.; Jalon, F. A.; Manzano, B. R. *J. Chem. Soc., Chem. Commun.* **1998**, 1879.

(17) Scharrer, E.; Chang, S.; Brookhart, M. *Organometallics* **1995**, *14*, 5686–5694.

Scheme 1



Scheme 2



in an iron dihydride which isomerized to a dihydrogen complex upon warming. Loss of H_2 above 10°C precluded isolation of the iron dihydrogen complex. This is the only example in the literature of the kinetic site of protonation being the metal despite the thermodynamic site being the hydride ligand. Therefore, the kinetic preference for hydride ligand protonation is very strong, and a unique combination of steric and electronic factors are needed to reverse this preference.

We decided to search for a dihydrogen intermediate in the protonation of $\text{CpW}(\text{CO})_2(\text{PMe}_3)\text{H}$ (**3**), known eventually to form the cationic dihydride $([\text{CpW}(\text{CO})_2(\text{PMe}_3)\text{H}_2]^+)$ (**4**). This system had the advantage over those previously studied in that both **3** and **4** had been fully characterized. The hydride complex **3** was first synthesized in 1970 and identified by ^1H and ^{31}P NMR and IR spectroscopy, and exists in solution in both cis (**3c**) and trans (**3t**) forms which interconvert rapidly on the NMR time scale (Scheme 1).¹⁸ The structure of the cationic dihydride **4** has been determined by X-ray diffraction.¹⁹ The hydride ligands of the cationic dihydride **4** interconvert rapidly at room temperature, and two inequivalent hydride resonances are not observed until the temperature is lowered to -112°C .²⁰

If the kinetic site of protonation of **3** is the hydride ligand, H/D exchange between the hydride complex **3** and an acid will occur faster than protonation of the W to form the dihydride cation **4** (Scheme 2). We have therefore compared the rate of H/D exchange between **3** and various acids with the rate at which these acids protonate the metal.

Experimental Section

General. All manipulations were carried out using Schlenk, high-vacuum, or inert-atmosphere-box techniques, unless otherwise indicated. $\text{CpW}(\text{CO})_2(\text{PMe}_3)\text{H}$ (**3**) was prepared by a literature procedure.²¹ $\text{CpW}(\text{CO})_2(\text{PMe}_3)\text{D}$ (**3-d**) (90% D) was formed via reaction of **3** with KH, followed by quenching with CF_3COOD . $([\text{CpW}(\text{CO})_2(\text{PMe}_3)\text{H}_2][\text{BF}_4])$ (**4a**) was formed by treating **3** with $\text{HBF}_4\cdot\text{OME}_2$.²⁰

$([\text{PhNH}_3^+(\text{OEt}_2)_{1-2}][\text{B}(\text{Ar}^f)_4])$ was prepared by treating $([\text{H}(\text{OEt}_2)_2][\text{B}(\text{Ar}^f)_4])$ [$\text{Ar}^f = 3,5\text{-C}_6\text{H}_3(\text{CF}_3)_2$]²² with PhNH_2 in ether. $([\text{CpWH}_2(\text{CO})_2\text{PMe}_3][\text{B}(\text{Ar}^f)_4])$ (**4b**) was similarly prepared by treating $([\text{H}(\text{OEt}_2)_2][\text{B}(\text{Ar}^f)_4])$ [$\text{Ar}^f = 3,5\text{-C}_6\text{H}_3(\text{CF}_3)_2$]²² with **3** in CH_2Cl_2 . 4-*tert*-Butyl-*N,N*-dimethylaniline (**6**) was distilled from sodium and treated with $\text{HBF}_4\cdot\text{OME}_2$ in ether to form the anilinium tetrafluoroborate (**5**), which was recrystallized from CH_2Cl_2 and hexane. The deuterated acid (**5-d**) was prepared by repeated exchange of **5** with EtOD , yielding 97% D incorporation. The chloride salt of **5** was prepared by treating **6** with HCl /ether, followed by ether removal under vacuum. 4-*tert*-

(18) Kalck, P.; Pince, R.; Poiblan, R.; Roussel, J. *J. Organomet. Chem.* **1970**, *24*, 445–452.

(19) Bullock, R. M.; Song, J. S.; Szalda, D. *J. Organometallics* **1996**, *15*, 2504–2516.

(20) Ryan, O. B.; Tilset, M.; Parker, V. D. *J. Am. Chem. Soc.* **1990**, *112*, 2618–2626.

(21) (a) Tate, D. P.; Knipple, W. R.; Augl, J. M. *Inorg. Chem.* **1962**, *1*, 433–434. (b) Keppie, S. A.; Lappert, M. F. *J. Chem. Soc. (A)* **1971**, 3216–3220. (c) Kalck, P.; Poiblan, R. *J. Organomet. Chem.* **1969**, *19*, 115–121.

(22) Brookhart, M. S.; Grant, B.; Volpe, A. F. *Organometallics* **1992**, *11*, 3920–3922.

Table 1. H/D Exchange between **3** and **5**

[5- <i>d</i> ₁] (M) ^a	[3] (M) ^a	[5] (M) ^a	[3-d ₁] (M) ^a	<i>T</i> (K) ^b	<i>k</i> _f (M ⁻¹ s ⁻¹) ^c	<i>k</i> _r (M ⁻¹ s ⁻¹) ^c	<i>R</i> ^c	<i>K</i> _{eq} ^d
0.061	0.051	0	0	283	8.1 × 10 ⁻⁴	4.2 × 10 ⁻³	0.006	0.19
0.116	0.058	0	0	293	1.5 × 10 ⁻³	8.8 × 10 ⁻³	0.01	0.17
0.117	0.053	0	0	293	1.8 × 10 ⁻³	9.4 × 10 ⁻³	0.01	0.2
0	0	0.105	0.051	273	3.6 × 10 ⁻⁴	1.7 × 10 ⁻³	0.04	0.21
0	0	0.104	0.048	263	1.9 × 10 ⁻⁴	1.0 × 10 ⁻³	0.02	0.19
0	0	0.127	0.058	283	7.5 × 10 ⁻⁴	4.3 × 10 ⁻³	0.01	0.18
0	0	0.127	0.055	283	8.4 × 10 ⁻⁴	4.6 × 10 ⁻³	0.01	0.18

^a Initial concentrations. ^b Temperature at which kinetics were monitored. ^c Determined by MacKinetics. ^d *K*_{eq} = *k*_f/*k*_r.

Table 2. Stopped-Flow Kinetics of Deprotonation of **4a**

[6] (M)	<i>k</i> _{r mp} (223 K ^c , s ⁻¹)	<i>k</i> _{r mp} (233 K ^c , s ⁻¹)	<i>k</i> _{r mp} (243 K ^c , s ⁻¹)	<i>k</i> _{r mp} (253 K ^c , s ⁻¹)	<i>k</i> _{r mp} (263 K ^c , s ⁻¹)
0.00511 ^a		9.2(4)	16.3(5)	29(3)	50(3)
0.00652 ^b	4.5(3)	11.0(9)	21(3)	34(3)	66(6)
0.00835 ^b	6.1(3)	12(1)	25(2)	42(5)	77(8)
0.0102 ^b				53(5)	

^a Four kinetic runs were done at each temperature. ^b Between 9 and 11 kinetic runs were done at each temperature. ^c Represents the average temperature; the true temperature used in extracting kinetic data was within 1 K of this value.

Butyl-*N,N,N*-trimethylanilinium tetrafluoroborate was prepared by a variation of a literature method;²³ **6** was treated with [Me₃O][BF₄] in CH₂Cl₂, followed by precipitation with hexanes. The tetrafluoroborate salts of 2,4-dichloroanilinium, 4-cyanoanilinium, and 4-carboethoxyanilinium were prepared by treating HBF₄·OMe₂ with the corresponding aniline in ether, followed by recrystallization from ethanol and drying under vacuum.

CH₃CN and CD₃CN were purified by a series of steps that our previous work had shown to be effective;^{24,25} they were first treated with anhydrous cupric sulfate to remove amines; then, they were fractionally distilled from P₄O₁₀, discarding the first 5–10% of the distillate to remove acrylonitrile; last, they were distilled from CaH₂, again discarding the first 5% of the distillate. Et₂O, THF, and hexanes were distilled under N₂ from sodium/benzophenone. CH₂Cl₂ and CD₂Cl₂ were distilled under N₂ from P₄O₁₀.

NMR. ¹H, ¹⁹F, and ¹³C NMR spectra and kinetic data were recorded on a Bruker 300-MHz instrument. Temperatures (223–283 K) were checked with a methanol thermometer;²⁶ the uncertainty in temperature was estimated to be ±1 K between 223 and 283 K. NMR line shape simulations were done with Chermwell Scientific's gNMR 4.1 software.

Kinetics of Cis/Trans Isomerization. ¹H NMR spectra of a CD₂Cl₂ solution of 0.065 M **3** were taken in 5 K increments from 268 to 298 K, and the rates were determined by line shape simulation.

H/D Exchange between **3 and Triflic Acid.** A CD₂Cl₂ solution (600 μL) of **3** (0.0742 M) was placed in a J. Young NMR tube and cooled at -80 °C. A separate vacuum bulb was charged with 2.7 μL of CF₃SO₃D, and the latter was vacuum transferred onto the hydride solution. ¹H NMR spectra were taken at 223 K; the progress of the reaction was observed by monitoring the hydride resonances (δ -7.9, **3t**; δ -8.0, **3c**; δ -2.5, **4a**).

Proton Exchange between **3 and [PhNH₃·(OEt)₂]₁₋₂[B(Ar^f)₄].** In a typical experiment, the ¹H NMR spectra of **3** (0.019 M) were examined in the presence of [PhNH₃·(OEt)₂]₁₋₂[B(Ar^f)₄] [Ar^f = 3,5-C₆H₃(CF₃)₂] (0.0084 M) in CD₂Cl₂ at 206–273 K. The exchange was monitored by observing the line broadening of the hydride resonances (δ -7.9, **3t**; δ -8.0, **3c**).

Deprotonation of [CpWH₂(CO)₂PMe₃][B(Ar^f)₄] (4b**).** ¹H NMR Line Widths of the Resulting **3**. In a typical experiment, a solution of **4b** (0.042 M) in CD₂Cl₂ and increasing amounts of PhNH₂ (0.014–0.087 M) were combined in a NMR tube. The trans hydride resonance was broadened into the baseline until the concentration of aniline was 0.087 M, at which point the rates of exchange and metal protonation of the resulting **3** were determined by observing the broadening of the hydride resonance (δ -7.9, **3t**; δ -8.0, **3c**) and the PMe₃ resonance (δ 1.63, **3t**; δ 1.59, **3c**) at 273 K. The relative rate constants for metal and hydride protonation were determined as described in the text.

H/D Exchange between **3 and **5**.** A CD₂Cl₂ solution (300 μL) of **5** (0.232 M) and C₆H₁₈O₃Si₃ (as an internal standard) (0.06 M) was placed in a septum-sealed NMR tube. A separate NMR tube was charged with

a CD₂Cl₂ solution of **3-d**₁ (0.104 M, 300 μL). The **3-d**₁ solution was transferred by cannula onto the anilinium solution, which was at -78 °C. An ¹H NMR spectrum was taken at 223 K to ensure that no exchange had taken place, and then the probe was warmed to an appropriate temperature (see Table 1). The progress of the reaction was observed by monitoring the hydride resonances (δ -7.9, **3t**; δ -8.0, **3c**). The forward and backward rate constants were obtained using MacKinetics²⁷ simulation software, with initial concentrations for all species and the time dependence of the tungsten hydride as input.

Stopped-Flow System. The variable-temperature stopped-flow system has been previously described.²⁸ One spectrum was taken each millisecond with an RSM 1000 monochromator, calibrated with holmium oxide. The photomultiplier tube output from the SF-41 was converted to digital form with an Analog Devices A/D converter and analyzed (on a Gateway 2000 Pentium PC) with OLIS-RSM software.

Kinetics of Deprotonation of **4a by **6**.** A CH₂Cl₂ solution of **4a** (1.18 × 10⁻³ M) was placed in one reservoir by syringe. The other reservoir was filled with a CH₂Cl₂ solution that contained an excess of **6** (1.71 × 10⁻² M). The reaction was monitored by observing the hydride absorbance at 346 nm. The aniline concentration and the temperature were varied in several experiments (see Table 2).

Raman Spectra. The spectra were obtained in vacuum-sealed NMR tubes containing crystals of **3c** and **3c-d**₁, using a 135° backscattering geometry and a triple-stage spectrograph (Spex Triplemate) equipped with a Princeton Instruments diode array detector. Excitation source was a Spectra Physics model 2020 Ar⁺ laser. The spectra were referenced with DMF and processed with Grams/32 software (Galactic Corp.).

X-ray Structure Determination of **3.** Crystals of **3** were grown from hexane at -30 °C. Single-crystal data collection and refinement parameters are summarized in Table 3. Data were collected on a Bruker P4 diffractometer equipped with a SMART CCD detector. The structure was solved using direct methods and standard difference map techniques and refined by full-matrix least-squares procedures using SHELXTL.²⁹ Hydrogen atoms on carbon were included in calculated positions.

Crystals of **3** were ground to a powder and sprinkled onto a Vaseline-coated glass lens, which was rotating during powder X-ray data

(23) Petti, M. A.; Sheppard, T. J.; Barrans, R. E., Jr.; Dougherty, D. A. *J. Am. Chem. Soc.* **1988**, *110*, 6825–6840.

(24) Moore, E. J.; Sullivan, J. M.; Norton, J. R. *J. Am. Chem. Soc.* **1986**, *108*, 2257–2263.

(25) (a) Burfield, D. R.; Lee, K. H.; Smithers, R. H. *J. Org. Chem.* **1977**, *42*, 3060–3065. (b) The authors thank Professor V. L. Pecoraro for suggesting distillation from CaH₂ to neutralize any acids present after the P₄O₁₀ treatment.

(26) Van Geet, A. L. *Anal. Chem.* **1970**, *42*, 679.

(27) McKinney, R. J.; Weiher, J. F.; Leipold, W. S. *MacKinetics*; E. I. du Pont de Nemours, Inc.: Wilmington, DE, 1992–1995.

(28) Eisenberg, D. C.; Lawrie, C. J. C.; Moody, A. E.; Norton, J. R. *J. Am. Chem. Soc.* **1991**, *113*, 4888–4895.

Table 3. Summary of Crystallographic Data of **3c**

empirical formula	C ₁₀ H ₁₅ O ₂ PW
formula weight	382.04
temperature, K	238(2)
crystal system	monoclinic
space group	<i>P</i> 2 ₁ / <i>c</i>
<i>a</i> , Å	8.3686(10)
<i>b</i> , Å	12.4131(14)
<i>c</i> , Å	12.1808(14)
α , deg	90
β , deg	105.602(2)
γ , deg	90
<i>V</i> , Å ³	1218.7(2)
<i>Z</i>	4
<i>D</i> _{calc} , g/cm ³	2.082
λ (Mo K α), Å	0.71073
μ , mm ⁻¹	9.584
no. of data collected	6920
no. of unique data	2684
data/restraints/param	2684/0/153
GOF on <i>F</i> ²	1.047
<i>R</i> 1, <i>wR</i> 2 (<i>I</i> > 2 σ (<i>I</i>))	0.0386, 0.1053
<i>R</i> 1, <i>wR</i> 2 (all data)	0.1143, 0.1462

Table 4. Determination of the CH₃CN p*K*_a(**4a**) from the Equilibrium between **3** and BH⁺

acid (BH ⁺)	p <i>K</i> _a (BH ⁺)	<i>K</i> _{eq}	p <i>K</i> _a (4a)
4-carboethoxyanilinium	8.2(1)	2.5 × 10 ⁻³	5.6(1)
4-cyanoanilinium (8-H ⁺)	7.6(1)	0.011	5.6(1)
2,4-dichloroanilinium (7-H ⁺)	7.0(2) ^a	0.029	5.5(1)

^a This p*K*_a had been previously reported as 8.0,³¹ but the observation of such a high *K*_{eq} between **3** and **7-H**⁺ led us to reinvestigate this p*K*_a.

collection. The radiation source was Cu K α , $\lambda_1 = 1.54060$ Å, $\lambda_2 = 1.54439$ Å, and data were collected from $2\theta = 1.025$ to 49.975 (Figure 2a). A calculated X-ray diffraction powder pattern of **3c** was obtained using X-Pro software.²⁹

Calculation of the Normal Modes of 5 and 5-d₁. These calculations were done for the gas-phase cations using Jaguar version 3.5, release 42, basis set 6-31G**.³⁰ These results were helpful in assigning the bending modes in the experimental IR spectra; see Supporting Information for details.

Determination of the CH₃CN p*K*_a of 4a. All p*K*_a determinations were done in CH₃CN using a CaF₂ cell. The equilibria between **3** and the three anilinium acids listed in Table 4 were observed by IR. For each acid used, the *K*_{eq} was determined from the absorbance of the ν_{CO} bands (**3** absorbs at 1919 and 1831 cm⁻¹, with known ϵ ;²⁴ **4a** absorbs at 2073 cm⁻¹ with $\epsilon = 1600$ M⁻¹ cm⁻¹ and at 2015 cm⁻¹ with $\epsilon = 1700$ M⁻¹ cm⁻¹). Two experiments at different starting acid concentrations were done with each acid.

Determination of the CH₃CN p*K*_a of 5. The equilibrium between **5** and pyridinium triflate was observed from the averaged ¹H NMR chemical shift of the aromatic protons of **5** and **6** in fast exchange during six experiments at different starting concentrations; see Supporting Information for details.

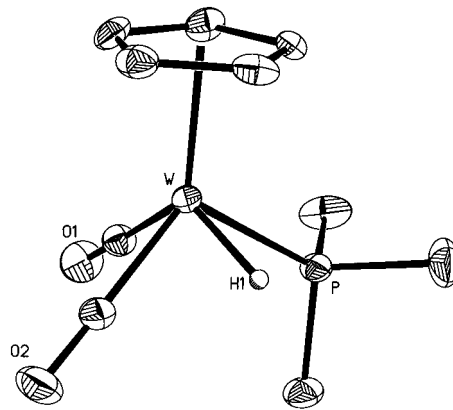
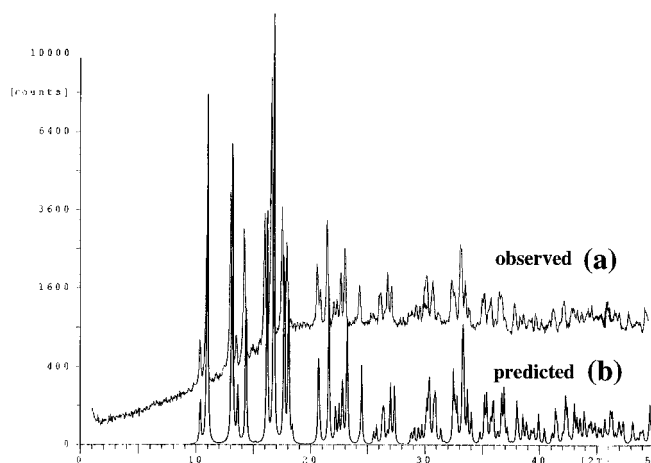
Redetermination of the CH₃CN p*K*_a of 2,4-Dichloroanilinium (7-H⁺). The equilibrium between **7-H**⁺ and 4-cyanoaniline (**8**) was observed from the averaged ¹H NMR chemical shift of the aromatic protons of **8** and **8-H**⁺ in fast exchange during two experiments at different starting concentrations; see Supporting Information for details.

Results and Discussion

Solid State Structure of CpWH(CO)₂PMe₃ (3). An X-ray structure of a single crystal of **3** revealed that the solid structure is cis, as shown in Figure 1. The hydrogen atoms were located and refined; the apparent W–H distance was 1.30(8) Å. From the single-crystal structure, a predicted powder pattern was

(29) Sheldrick, G. M. *SHELXTL*, An Integrated System for Solving, Refining and Displaying Crystal Structures from Diffraction Data; University of Göttingen, Göttingen, Federal Republic of Germany, 1981.

(30) Jaguar v. 4.0; Schrödinger, Inc.: Portland, OR, 1999.

**Figure 1.** Thermal ellipsoid plot of CpW(CO)₂PMe₃H (**3**).**Figure 2.** XRD powder pattern of **3** (Cu radiation): (a) experimental and (b) calculated.**Table 5.** Kinetics of Cis–Trans Isomerization of **3**

	<i>k</i> _{c→t}	<i>k</i> _{t→c}
ΔH^\ddagger (kcal/mol)	15.5(2)	15.4(3)
ΔS^\ddagger (eu)	−0.2(9)	0.2(1)
ΔG^\ddagger_{263K} (kcal/mol)	15.51(2) ^a	15.39(2) ^a
<i>k</i> _{263K} (s ⁻¹)	0.72(3) ^a	0.91(4) ^a

^a Extrapolated from rate measurements at 268–298 K.

obtained (Figure 2b) that agreed with the observed powder pattern of crystals of **3** (Figure 2a). Thus, in the solid phase, **3** is exclusively **3c**. Hence, the cis isomer of **3** preferentially crystallizes from the mixture of cis and trans isomers found in solution.

Rates of Cis/Trans Isomerization. In solution, **3c** and **3t** interconvert rapidly on the NMR time scale (Scheme 1). The published line shape analysis showed that the first-order rate of isomerization *k*_{cis→trans} of **3** is 4.62 s⁻¹ at 280 K in toluene-*d*₈.¹⁸ The kinetics of interconversion between **3c** and **3t** (Scheme 2) were redetermined by variable-temperature NMR in CD₂Cl₂ (a more practical solvent for proton-transfer reactions). Line shape analysis of the PMe₃ resonance ($\delta = 1.58$ ppm) gave the rate of cis–trans isomerization and the kinetic parameters found in Table 5. The activation parameters were very close to those found in toluene by Poiblanç et al. (*k*_{cis→trans} is 4.56 s⁻¹ at 280 K in CD₂Cl₂);¹⁸ a solvent effect is not expected for an intramolecular process. Above 263 K, the rate of cis/trans isomerization is sufficiently fast to maintain equilibrium between **3c** and **3t** throughout proton exchange with deuterated acid.

H/D Exchange between 3 and Triflic Acid. Since triflic acid is known to protonate **3**,¹⁹ we began our study of the

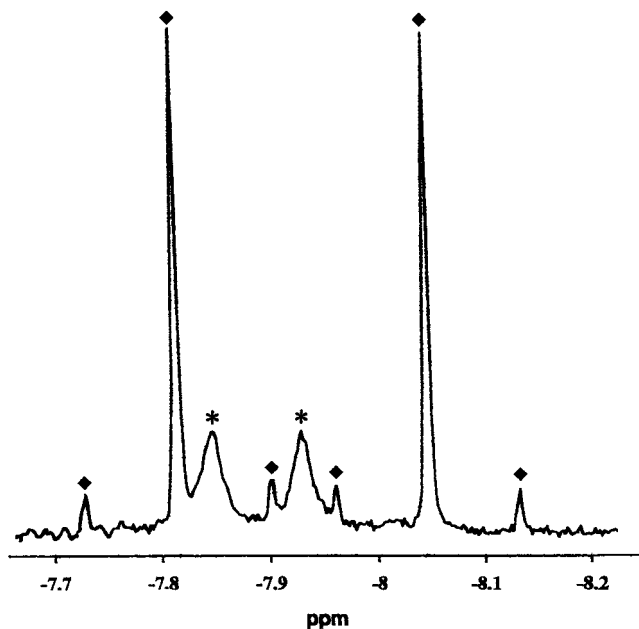


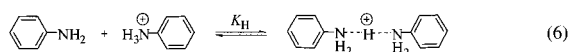
Figure 3. ¹H NMR of hydride region of **3** (0.019 M) broadened by exchange with [PhNH₃⁺(OEt₂)₁₋₂][B(Ar^f)₄]⁻ (0.0084 M) in CD₂Cl₂ at 263 K. Signals marked with * and ◆ are due to **3t** and **3c**, respectively.

protonation of **3** by examining the rate of isotopic exchange between **3** and TfOD. Preliminary NMR experiments in CD₂Cl₂ at 223 K showed that proton exchange was faster than addition of D⁺ (or H⁺) to the metal. However, both reactions proved to be too fast to quantify even at that temperature.

Proton Exchange between **3 and [PhNH₃⁺(OEt₂)₁₋₂][B(Ar^f)₄]⁻.** To slow both protonation reactions, and ideally to quantify their rates, the ¹H NMR spectrum of **3** was examined in the presence of [PhNH₃⁺(OEt₂)₁₋₂][B(Ar^f)₄]⁻ [Ar^f = 3,5-C₆H₃(CF₃)₂] (pK_a = 10.5 in acetonitrile³¹) in CD₂Cl₂. (The anion was chosen because it enhances solubility in CD₂Cl₂,²² and the ethers cocrystallized with the PhNH₃⁺ salt.) This acid protonated **3** to a small extent (no signal attributable to a dihydrogen complex was seen), and it gave *selective broadening of the hydride resonance of the trans hydride 3t* by ~7.5 Hz at 263 K (Figure 3).

This broadening is surely the result of *selective protonation of the hydride ligand of 3t*. There is no plausible reason for protonation at the metal to be faster for **3t** than for **3c**, while the hydride ligand of **3t** is known to be more reactive toward electrophiles than the hydride ligand of **3c**.^{4a,32}

Evidence of Aniline/Anilinium Homoconjugate Pair Formation. To check for interactions between PhNH₂ and PhNH₃⁺ in the preceding experiment, we plotted the average chemical shift of aniline and [PhNH₃⁺(OEt₂)₁₋₂][B(Ar^f)₄]⁻ versus aniline mole fraction in CD₂Cl₂ (Figure 4). A linear relationship would have indicated that no species other than PhNH₂ and PhNH₃⁺ were present. The nonlinear relationship observed in Figure 4 suggests extensive homoconjugate pair formation (eq 6). The



addition of ether varied the chemical shift of [PhNH₃⁺(OEt₂)₁₋₂][B(Ar^f)₄]⁻, implying that there are additional interactions between PhNH₃⁺ and Et₂O.

(31) (a) Edidin, R. T.; Sullivan, J. M.; Norton, J. R. *J. Am. Chem. Soc.* **1987**, *109*, 3945–3953. (b) Coetzee, J. F. *Prog. Phys. Org. Chem.* **1967**, *4*, 45.

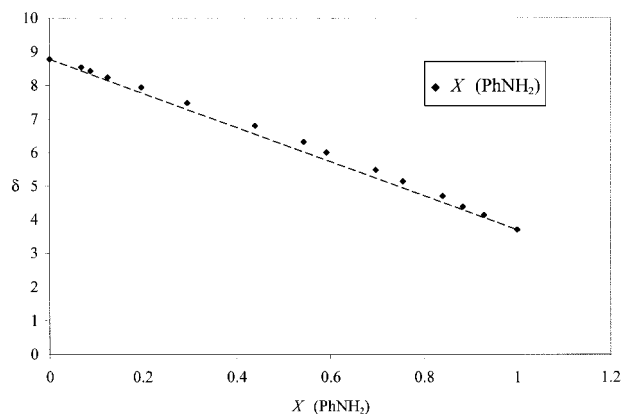
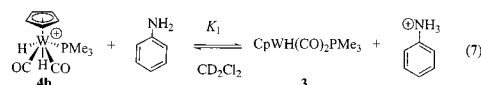


Figure 4. Plot of the average chemical shift of PhNH₂ and [PhNH₃⁺(OEt₂)₁₋₂][B(Ar^f)₄]⁻ (δ) versus mole fraction (X) of PhNH₂. A linear plot would indicate that homoconjugation is negligible.

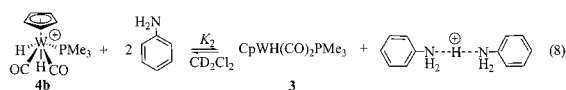
Effect of Added Aniline on Equilibrium between **3 and Anilinium.** When [PhNH₃⁺(OEt₂)₁₋₂][B(Ar^f)₄]⁻ was added to **3** in the presence of 1 equiv of PhNH₂, the formation of [CpWH₂(CO)₂PMe₃][B(Ar^f)₄]⁻ (Ar^f = 3,5-C₆H₃(CF₃)₂) (**4b**) was suppressed. From this point we will distinguish between **4a**, the BF₄⁻ salt of the cation **4**, and **4b**, the B(Ar^f)₄⁻ salt of **4**. The trans hydride signal still showed significant broadening relative to the signal of the cis isomer. However, because our PhNH₃⁺/Et₂O experiments had shown that ether was not an innocent spectator, it was impossible to deduce meaningful quantitative data from these exchange studies.

Deprotonation of [CpWH₂(CO)₂PMe₃][B(Ar^f)₄]⁻ (4b**) by Aniline.** To eliminate ether, **3** was generated by incomplete deprotonation of [CpWH₂(CO)₂PMe₃][B(Ar^f)₄]⁻ (**4b**) by aniline (eq 7). Separate signals were observed for **3**, **4b**, and the acidic



hydrogens of the solution. The hydride resonance of **3t** was broadened more (about 60 Hz) than its PMe₃ resonance (2 Hz) at 0 °C. The resulting first-order rate constants (6.5(7) s⁻¹ for metal protonation, 180(30) s⁻¹ for exchange) show that the hydride ligand is protonated more rapidly than the tungsten (conversion of **3** to **4b** will broaden both signals, but exchange will only broaden the hydride resonance).

PhNH₃⁺ is capable of protonating **3** only because of its strong interaction with its conjugate base, PhNH₂. The overall reaction is thus the combination of eqs 6 and 7 or eq 8, with equilibrium constant K₂ (eq 9).



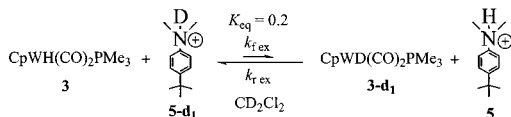
$$K_2 = K_1 K_H = \frac{[\mathbf{3}][\text{PhNH}_2 \cdots \text{H}^+ \cdots \text{H}_2\text{NPh}]}{[\mathbf{4b}][\text{PhNH}_2]^2} = \frac{[\mathbf{3}]^2}{[\mathbf{4b}]\{[\text{PhNH}_2]_0 - 2[\mathbf{3}]\}^2} \quad (9)$$

Note that [PhNH₂⋯H⁺⋯H₂NPh] = [3] and [PhNH₂] =

(32) For a discussion of the increased kinetic hydricity of trans and cis hydrides, see: Cheng, T. Y.; Brunschwig, B. S.; Bullock, R. M. *J. Am. Chem. Soc.* **1998**, *120*, 13121–13137.

Table 6. Kinetics of Proton Exchange between **3** and **5-d₁**

	$k_{f\text{ex}}$	$k_{r\text{ex}}$
ΔH^\ddagger (kcal/mol)	10.7(5)	11.2(6)
ΔS^\ddagger (eu)	-35(2)	-30(2)
$\Delta G^\ddagger_{263\text{K}}$ (kcal/mol)	19.86(4)	19.01(4)
$k_{263\text{K}}$ ($\text{M}^{-1} \text{s}^{-1}$)	$1.8(1) \times 10^{-4}$	$8.9(8) \times 10^{-4}$

Scheme 3

[PhNH₂]₀ - 2[**3**]. A plot of ([PhNH₂]₀ - 2[**3**])² versus ([**3**]/[**4b**]) is linear (Figure S-1, Supporting Information) with slope $K_2 = K_1K_H = 88.3(4) \text{ M}^{-1}$. Unfortunately, K_H is unknown in CD₂Cl₂, so it is not possible to quantify K_1 from this experiment or to estimate the value of $\text{p}K_a(\mathbf{4b})$ in any solvent.

Homoconjugate pair formation also makes it impossible to obtain from the line-broadening experiments a meaningful second-order rate constant for either reaction (exchange or protonation at the metal) of **3t**. The nature and concentration of the effective acids are uncertain.

¹H NMR Spectrum of 3 in the Presence of 4-tert-Butyl-N,N-dimethylanilinium Tetrafluoroborate (5). To eliminate homoconjugate pair formation, we then tried a dimethyl-substituted anilinium salt. A *tert*-butyl substituent enhanced solubility in CD₂Cl₂ so that tetrafluoroborate could be used as a counteranion and a smaller mass of acid was required for the concentrations desired. The ¹H NMR spectrum of **3** was little affected by the presence of varying amounts of **5** at temperatures from 300 to 223 K, although slight broadening of the hydride peaks (<1 Hz) was observed. The line width and chemical shift changes were much smaller than those observed when there is hydrogen bonding between hydride ligands and acids.³³ Furthermore, similar line broadening and chemical shift changes were observed in the presence of 4-*tert*-butyl-*N,N,N*-trimethylanilinium tetrafluoroborate, which has no acidic protons; the slight effect of **5** on the ¹H NMR spectrum of **3** thus arose from a nonspecific ionic interaction. No differential broadening by **5** of the hydride resonance of **3t** relative to that of **3c** was observed. As subsequent experiments showed, H/D exchange between **3** and **5** is too slow to cause line broadening.

H/D Exchange Between 3 and 5. Table 6 summarizes the results of ¹H NMR studies in CD₂Cl₂ of the isotope exchange in Scheme 3; as expected, no metal protonation was observed. Seven experiments were done (Table 1), starting from both sides of the equilibrium. The activation parameters are summarized in Table 6; ΔH^\ddagger is ~ 11 kcal/mol; ΔS^\ddagger is ~ -30 eu, as expected for a bimolecular process; ΔG^\ddagger is ~ 19 kcal/mol at 263 K. Values of K_{eq} were calculated from the ratio of $k_{f\text{ex}}/k_{r\text{ex}}$ as well as from the final integrated intensities. K_{eq} was consistently found to be 0.19(2), a surprisingly large equilibrium isotope effect (EIE).

Calculation from their Vibrational Frequencies of the EIE To Be Expected for H/D Exchange between 3 and 5. While equilibrium isotope effects can be calculated from a knowledge of the vibrational frequencies of all species involved,³⁴ such a calculation is complicated in the case of the equilibrium in Scheme 3 by the fact that **3** in solution is a mixture of **3t** and

Table 7. Experimental Vibrational Modes of **3c**, **3c-d₁**, **5**, and **5-d₁**

	$\nu_{\text{WH}}(\mathbf{3})$ (cm^{-1})	$\nu_{\text{WD}}(\mathbf{3-d}_1)$ (cm^{-1})	$\nu_{\text{NH}}(\mathbf{5})$ (cm^{-1})	$\nu_{\text{ND}}(\mathbf{5-d}_1)$ (cm^{-1})
stretching	1850 ^a	1322 ^a	3117 ^b	2320 ^b
bending	539 ^a	472 ^a	1482 ^c	1016 ^c
bending	456 ^a	381 ^a	1183 ^c	1062 ^c

^a From the Raman spectra of crystalline **3c** and **3c-d₁**. ^b From the IR spectra of **5** and **5-d₁** in CH₂Cl₂ in a KBr cell. ^c From the IR spectra of 4-*tert*-butyl-*N,N*-dimethylanilinium chloride and 4-*tert*-butyl-*N,N*-dimethylanilinium-*N-d₁* chloride in CH₃CN in a KBr cell (the chloride salts were not soluble in CH₂Cl₂). These bending modes could not be located in **5** and **5-d₁** due to strong B-F stretches from 1150 to 950 cm^{-1} .

3c. While IR spectra of **3** in solution would thus give the vibrational frequencies of **3t** along with those of **3c**, the Raman spectrum of crystalline **3** (shown above to be exclusively **3c**) gives the vibrational frequencies of **3c** only. We have thus given only the stretching and bending modes of the H and D ligands of **3c** and **3c-d₁** in Table 7—clearly identifiable from the Raman spectra. The frequencies of the normal modes of **3t** are probably similar to those of **3c**; their carbonyl stretches differ by less than 10 cm^{-1} .¹⁸

A theoretical calculation of the normal modes for **5** and **5-d₁** gas-phase cations showed that we should expect one stretch and two bends. The condensed-phase spectra showed additional peaks, so the Teller-Redlich product rule and the frequencies of the calculated bending modes (see Supporting Information) were used to select the experimental frequencies given in Table 7. These were used along with the vibrational frequencies of **3c** and **3c-d₁** to estimate an EIE value.

There is precedent³⁵ for using only the W-H(D) and N-H(D) stretching frequencies to estimate K_{eq} (eq 10). The N-H, N-D, W-H, and W-D frequencies, as shown in Table 3, were 3117, 2320, 1850, and 1322 cm^{-1} , respectively, suggesting a K_{eq} of 0.50 at 283 K.

$$K_{\text{eq}} \approx \text{ZPE}(\text{stretching modes})$$

$$= \exp\{-(hc/2k_B T)(\nu_{\text{WH}} - \nu_{\text{WD}} - \nu_{\text{NH}} + \nu_{\text{ND}})\} \quad (10)$$

Of course, eq 10 does not consider all normal modes of the reactants and products. A more complete description of equilibrium isotope effects (EIEs) can be found in eqs 11–13,^{34,36} which consider all isotopically sensitive normal modes.

$$\text{EIE} = k_{f\text{ex}}/k_{r\text{ex}} = K_{\text{eq}} = \text{MMI} \times \text{EXC} \times \text{ZPE} \approx \text{EXC} \times \text{ZPE} \quad (11)$$

$$\text{EXC} = \prod_i^{3N_r - 6} \frac{1 - e^{-hc\nu_i^{\text{WH}}/k_B T}}{1 - e^{-hc\nu_i^{\text{WD}}/k_B T}} \bigg/ \prod_j^{3N_p - 6} \frac{1 - e^{-hc\nu_j^{\text{NH}}/k_B T}}{1 - e^{-hc\nu_j^{\text{ND}}/k_B T}} \quad (12)$$

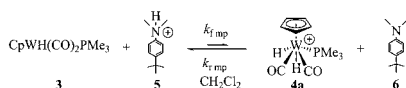
$$\text{ZPE} = \prod_i^{3N_r - 6} \frac{e^{hc\nu_i^{\text{WH}}/k_B T}}{e^{hc\nu_i^{\text{WD}}/k_B T}} \bigg/ \prod_j^{3N_p - 6} \frac{e^{hc\nu_j^{\text{NH}}/k_B T}}{e^{hc\nu_j^{\text{ND}}/k_B T}} \quad (13)$$

The EIE is the product of three factors: the rotational and translational factor, MMI, is close to unity and can be ignored; the EXC factor contains contributions from vibrational excited states and is also close to unity; the ZPE factor takes into account

(33) (a) Crabtree, R. H. *J. Organomet. Chem.* **1998**, *577*, 111–115. (b) Ayllon, J. A.; Gervaux, C.; Sabo-Etienne, S.; Chaudret, B. *Organometallics* **1997**, *16*, 2000–2002. (c) Shubina, E. S.; Belkova, N. V.; Krylov, A. N.; Vorontsov, E. V.; Epstein, L. M.; Gusev, D. M.; Niedermann, M.; Berke, H. *J. Am. Chem. Soc.* **1996**, *118*, 1105–1112.

(34) (a) Bender, B. R. *J. Am. Chem. Soc.* **1995**, *117*, 11239–11246. (b) Bender, B. R.; Kubas, G. J.; Jones, L. H.; Swanson, B. I.; Eckert, J.; Capps, K. B.; Hoff, C. D. *J. Am. Chem. Soc.* **1997**, *119*, 9179–9190. (c) Abul-Hasanayn, F.; Krogh-Jespersen, K.; Goldman, A. S. *J. Am. Chem. Soc.* **1993**, *115*, 8019–8023. (d) Rabinovich, D.; Parkin, G. *J. Am. Chem. Soc.* **1993**, *115*, 353–354.

Scheme 4



the differences in ground-state vibrational energy between the reactants and the products and accounts for the bulk of the EIE.³⁴

Inclusion of the one stretching frequency and two bending frequencies for compounds **3c**, **3c-d₁**, **5**, and **5-d₁** listed in Table 7 leads to a calculated EIE of 0.18 at 283 K, in excellent agreement with the experimentally observed EIE of 0.19. Since the bending modes of the H(D) ligand of **3** are much lower in frequency than those of the H(D) on the nitrogen in **5**, the stretching frequencies alone do not account for the EIE. (The relative energy difference in bending frequencies between **3** and **5** may be atypical of other EIEs, because the bending modes of **3** appear to be lower compared to those of other hydride complexes.)

Determination of the Rate Constant for 3 → 4a from the Equilibrium Constant and the Rate Constant for 4a → 3. As only triflic acid had proven strong enough to protonate the W of **3** (the rate of that protonation had proven too fast to measure) and protonation by anilinium introduced the complication of homoconjugation, we set out to determine the rate constant for protonation by **5** of the W of **3** ($k_{f\text{ mp}}$) from the equilibrium constant ($K_{\text{eq mp}}$) and the reverse rate constant ($k_{r\text{ mp}}$) (Scheme 4 and eq 14).

$$K_{\text{eq mp}} = k_{f\text{ mp}}/k_{r\text{ mp}} = K_{\text{a}}(\mathbf{5})/K_{\text{a}}(\mathbf{4a}) \quad (14)$$

Determination of the CH₃CN pK_a of 4a. An early estimate placed $\text{p}K_{\text{a}}(\mathbf{4a}) > 8.9$, from the observation that 5 equiv of dry HCl ($\text{p}K_{\text{a}} = 8.9$ in CH₃CN^{31b}) was able to protonate **3**.²⁰ However, HCl is a more effective acid than its $\text{p}K_{\text{a}}$ implies, because of homoconjugate pair formation between HCl and Cl⁻;²⁴ Co(CO)₄⁻ is protonated by HCl although the $\text{p}K_{\text{a}}$ of HCo(CO)₄ is 8.3.²⁴

In the absence of homoconjugate pair formation, the hydride **3** proved to be surprisingly difficult to protonate: it took 5 equiv of 4-cyanoanilinium to protonate 10% of **3**. The $\text{p}K_{\text{a}}$ of **4a** was determined by observing the protonation equilibria between **3** and three anilinium acids by IR, as shown in Table 4. (Homoconjugate pair formation is negligible in CH₃CN for such weakly basic anilines.)³⁷ Measurements with three different anilinium acids placed the CH₃CN $\text{p}K_{\text{a}}$ of **4a** at 5.6(1).

The pK_a of 5 in CH₃CN. The equilibrium between **6** and pyridinium triflate (CH₃CN $\text{p}K_{\text{a}} = 12.3$ ³⁸) was observed by NMR in CH₃CN, and $\text{p}K_{\text{a}}(\mathbf{5})$ was found to be 12.2(1). The known³⁹ $K_{\text{f}}[\text{py}_2\text{H}^+] = 7.0$ was used to correct for homoconjugate pair formation between pyridine (py) and pyridinium (pyH⁺).⁴⁰ The observed $\text{p}K_{\text{a}}(\mathbf{5})$ agrees with the estimate of 12.65 that can

(35) (a) Bullock, R. M.; Headford, C. E. L.; Hennessy, K. M.; Kegley, S. E.; Norton, J. R. *J. Am. Chem. Soc.* **1989**, *111*, 3897–3908. (b) Wolfsberg, M. *Acc. Chem. Res.* **1972**, *5*, 225. (c) Ritchie, C. D. *Physical Organic Chemistry: The Fundamental Concepts*; Marcel Dekker: New York, 1975; Chapter 8. (d) Lowry, T. H.; Richardson, K. S. *Mechanism and Theory in Organic Chemistry*, 3rd ed.; Harper: New York, 1987; p 255.

(36) (a) McLennan, D. J. In *Isotopes in Organic Chemistry*; Buncl, E., Lee, E., Eds.; Elsevier: New York, 1987; Vol. 7, Chapter 6, p 395. (b) Melander, L.; Saunders, W. H. *Reaction Rates of Isotopic Molecules*; Wiley: New York, 1980; p 20.

(37) Homoconjugate pair formation is negligible in CH₃CN for other anilinium acids with $\text{p}K_{\text{a}} < 8$ in CH₃CN; see: Izutsu, K. *Acid-Base Dissociation Constants in Dipolar Aprotic Solvents*; Blackwell Scientific Publications: Oxford, 1990.

(38) Coetzee, J. R.; Padmanabhan, G. *J. Am. Chem. Soc.* **1965**, *87*, 5005.

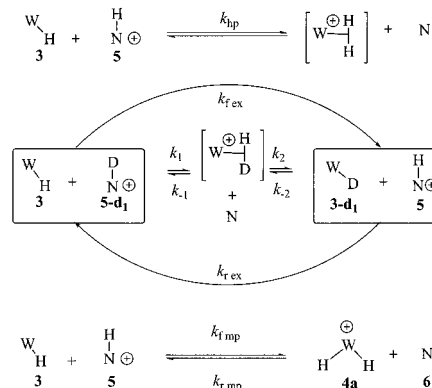
(39) Chantooni, M. K.; Kolthoff, I. M. *J. Am. Chem. Soc.* **1968**, *90*, 3005.

Table 8. Kinetics of Deprotonation of **4a** by **6**

	$k_{r\text{ mp}}$	$k_{f\text{ mp}}^a$
ΔH^\ddagger (kcal/mol)	7.0(2)	16.1(2) ^a
ΔS^\ddagger (eu)	-13.3(8)	-13.3(8) ^a
$\Delta G^\ddagger_{263\text{K}}$ (kcal/mol)	10.55(2)	19.57(2) ^a
$k_{263\text{K}}$ (M ⁻¹ s ⁻¹)	$9.5(3) \times 10^3$	$2.8(1) \times 10^{-4}$

^a Extrapolated from $k_{f\text{ mp}} = K_{\text{eq mp } 263\text{K}} k_{r\text{ mp}}$.

Scheme 5



be made from the aqueous $\text{p}K_{\text{a}}$ (5.15⁴¹) of *N,N*-dimethylanilinium (the difference between the CH₃CN $\text{p}K_{\text{a}}$ of anilinium ions and their aqueous $\text{p}K_{\text{a}}$ is approximately 7.5).¹

Kinetics of Deprotonation of 4a by 4-tert-Butyl-*N,N*-dimethylaniline (6). The formation of **3** and **5** from **4a** and **6** (rate constant $k_{r\text{ mp}}$) was monitored under pseudo-first-order conditions (excess of **6**) by stopped flow at low temperatures in CH₂Cl₂. The reaction proved quite rapid and first order in **6**.⁴²

The K_{a} values determined at room temperature (as described in the preceding section) give (eq 15) a $K_{\text{eq mp}}$ in CH₃CN at 300 K of 3.98×10^6 . If we assume that an equilibrium constant for proton transfer between two large bases should not vary appreciably from CH₃CN to CH₂Cl₂,⁴³ and correct $K_{\text{eq mp } 300\text{K}}$ to $K_{\text{eq mp } 263\text{K}}$ by assuming that the variation of ΔG_{mp} with temperature is negligible, then $k_{f\text{ mp}}$ in CH₂Cl₂ can be calculated from eq 15 (see Scheme 4 and Table 8).

$$K_{\text{eq mp } 263\text{K}} = k_{f\text{ mp}}/k_{r\text{ mp}} = \exp\{(300\text{K}/263\text{K}) \ln(K_{\text{eq mp } 300\text{K}})\} \quad (15)$$

Comparison of the Rate of Metal Protonation with That of Hydride Protonation.

To compare the second-order rate constant for metal protonation, $k_{f\text{ mp}}$, with that for hydride protonation, k_{hp} (as defined in Scheme 5), we must calculate the latter from $k_{f\text{ ex}}$. The rate of hydride protonation, k_{hp} , is related to $k_{f\text{ ex}}$ by a primary isotope effect on H(D)⁺ transfer to W–H from the anilinium ion and by the fractional probability F that formation of W(H–D)⁺ will result in detectable rearrangement (to W–D and N–H⁺).

(40) The averaged aromatic chemical shift of **5** and **6** in CD₃CN, observed by ¹H NMR, gave a linear relationship between δ and mole fraction of **6** (X_6) (see Supporting Information for more details), so homoconjugation is negligible—as expected in view of the methyl substituents.

(41) Serjeant, E. P.; Dempsey, B. *Ionization Constants of Organic Acids in Aqueous Solution*; Pergamon: Oxford, 1979.

(42) We have assumed that the stopped-flow experiments—which involve substantial concentrations of the base, **6**—measure the rate at which a proton is removed directly from **4a**. We have not observed the saturation kinetics (in **6**) that would have indicated deprotonation via an intermediate dihydrogen complex.

(43) Jia, G.; Morris, R. H. *Inorg. Chem.* **1990**, *29*, 581–582.

If secondary isotope effects are neglected, the ratio k_{-2}/k_1 can be estimated from the zero-point energies of the N–H and N–D bonds by assuming a linear transition state for proton transfer (eq 16).^{31a,44} K_{eq} and k_{-2}/k_1 can be used to estimate F in eqs 17–19. At 263 K, a temperature at which both $k_{\text{f ex}}$ and $k_{\text{r mp}}$ were measured, this gives $k_{\text{hp}} = 2.7 \times 10^{-3} \text{ M}^{-1} \text{ s}^{-1}$ and $k_{\text{f mp}} = 2.8 \times 10^{-4} \text{ M}^{-1} \text{ s}^{-1}$ from eqs 20 and 21, respectively. On this basis, hydride protonation is 9.6 times faster than metal protonation.

$$k_{-2}/k_1 = \exp\{(hc/2k_{\text{B}}T)(\nu_{\text{NH}} - \nu_{\text{ND}})\} = 8.9 \quad (16)$$

$$K_{\text{eq}} = k_1 k_2 / (k_{-1} k_{-2}) = 0.19 \quad (17)$$

$$F = k_2 / (k_{-1} + k_2) \quad (18)$$

$$1/F = 1 + k_{-1}/k_2 = 1 + (1/(K_{\text{eq}} k_{-2}/k_1)) = 1.6 \quad (19)$$

$$\begin{aligned} k_{\text{hp}} &= k_{\text{f ex}}(1/F)(k_{\text{H}}/k_{\text{D}}) = (1.8 \times 10^{-4} \text{ M}^{-1} \text{ s}^{-1})(1.6)(8.9) \\ &= 2.7 \times 10^{-3} \text{ M}^{-1} \text{ s}^{-1} \end{aligned} \quad (20)$$

$$\begin{aligned} k_{\text{f mp}} &= k_{\text{r mp}} K_{\text{eq mp}} = (9500 \text{ M}^{-1} \text{ s}^{-1})(3.0 \times 10^{-8}) \\ &= 2.8 \times 10^{-4} \text{ M}^{-1} \text{ s}^{-1} \end{aligned} \quad (21)$$

Conclusion

In CH_3CN , the protonation of $\text{CpW}(\text{CO})_2(\text{PMe}_3)\text{H}$ (**3**) is difficult ($\text{p}K_{\text{a}} = 5.6$), with 5 equiv of 4-cyanoanilinium capable of generating only 10% of the dihydride cation (**4a**). In CD_2Cl_2 the situation is quite different, with $[\text{PhNH}_3^+(\text{OEt}_2)_{1-2}][\text{B}(\text{Ar}^f)_4]$ capable of protonating some **3** because of the strong homoconjugate interaction between the resulting PhNH_2 and additional PhNH_3^+ . The change in the extent of protonation as the solvent is varied emphasizes the extent to which protonation equilibria in nonionizing solvents are affected by secondary interactions among the acids and bases present.

(44) Cheng, T. Y.; Bullock, R. M. *J. Am. Chem. Soc.* **1999**, *121*, 3150–3155.

Homoconjugate interaction can be prevented by using 4-*tert*-butyl-*N,N*-dimethylaniline (**6**) and 4-*tert*-butyl-*N,N*-dimethylanilinium tetrafluoroborate (**5**) instead of PhNH_2 and $[\text{PhNH}_3^+(\text{OEt}_2)_{1-2}][\text{B}(\text{Ar}^f)_4]$. Isotopic exchange between $\text{CpW}(\text{CO})_2(\text{PMe}_3)\text{H}$ (**3**) and 4-*tert*-butyl-*N,N*-dimethylanilinium (**5**) shows an equilibrium isotope effect (EIE) larger than expected on the basis of the stretching frequencies. Inclusion of the bending modes in the EIE calculation rationalizes the experimental value. From the forward and backward rate constants for exchange, $k_{\text{f ex}}$ and $k_{\text{r ex}}$, the rate of hydride protonation, k_{hp} , can be estimated.

The CH_3CN $\text{p}K_{\text{a}}$ of **5** and of **4a**, and the measured rate constant $k_{\text{r mp}}$ for the deprotonation of **4a** by **6** in CH_2Cl_2 , make it possible to estimate the rate constant $k_{\text{f mp}}$ for protonation at the metal by **5**. While some uncertainty is introduced by using the CH_3CN value of the proton-transfer equilibrium constant $K_{\text{eq mp}}$ in CH_2Cl_2 ,⁴⁵ $k_{\text{f mp}}$ appears to be an order of magnitude smaller than k_{hp} , the rate constant for hydride protonation.

Confirmation that the kinetic site of protonation for $\text{CpW}(\text{CO})_2(\text{PMe}_3)\text{H}$ is the hydride ligand is offered by the line widths in an equilibrium mixture of **3**, **4a**, and $[\text{PhNH}_2 \cdots \text{H}^+ \cdots \text{H}_2\text{NPh}]$. The line width of **3t**, and thus the first-order rate constant for exchange, is 27.5 times larger than that for metal protonation.

Acknowledgment. The authors thank the NSF for financial support (Grant CHE-99-7446) and Dr. B. R. Bender, Dr. G. Kaminsky, Dr. B. Bridgewater, Dr. C. J. Harlan, G. P. Abramo, J. P. Roth, A. Hanley, and Profs. L. Brammer, R. Friesner, and A. K. Rappé for helpful discussions and assistance with experiments.

Supporting Information Available: Experimental details from the determination of the CH_3CN $\text{p}K_{\text{a}}$ of **5**, redetermination of the CH_3CN $\text{p}K_{\text{a}}$ of 2,4-dichloroanilinium (**7-H**⁺), assignment of the isotopically dependent normal modes of **5** and **5-d**₁, linear plot to determine K_2 for deprotonation of $[\text{CpWH}_2(\text{CO})_2\text{PMe}_3][\text{B}(\text{Ar}^f)_4]$ (**4b**) by aniline, and structural data for $\text{CpWH}(\text{CO})_2\text{PMe}_3$ (**3c**) (PDF). This material is available free of charge via the Internet at <http://pubs.acs.org>.

JA002395S

(45) If $K_{\text{eq mp}}$ is in error by 150%, hydride protonation is still faster by at least a factor of 3.